Ocean Engineering 123 (2016) 45–54

Contents lists available at ScienceDirect

Ocean Engineering

journal homepage: www.elsevier.com/locate/oceaneng

Adaptive sliding-mode attitude control for autonomous underwater vehicles with input nonlinearities ☆

Rongxin Cui *, Xin Zhang, Dong Cui

School of Marine Science and Technology, Northwestern Polytechnical University, Xi'an 710072, PR China

ARTICLE INFO

Article history:
Received 18 June 2015
Received in revised form
27 May 2016
Accepted 28 June 2016

Keywords:
AUV
Adaptive sliding mode control
Anti-Windup
Dynamic compensator
Input nonlinearity

ABSTRACT

In this paper, we consider attitude control for autonomous underwater vehicles (AUVs) with input nonlinearities and unknown disturbances taken into account. The dynamics model in the 3D space of an AUV is simplified to a second-order dynamics with unknown model parameters and disturbances for the yaw and pitch control. Based on this simplification, a sliding-mode-based adaptive control is proposed for the case without any input nonlinearities. For the dead-zone nonlinearity and unknown disturbances, a sliding-mode-based adaptive control combined with a nonlinear disturbance observer is employed, in which the non-symmetric dead-zone with unknown parameters is modeled as a time-varying disturbance-like term rather than constructing a smooth dead-zone inverse. For rudder saturation, the control is further designed by introducing an auxiliary dynamic compensator. The mathematical proof of the proposed algorithms is presented. Extensive simulation results are presented to illustrate the effectiveness of the proposed control. In addition, experimental results on an AUV whose attitude is controlled by cross-type rudders are also provided to show the effectiveness of the proposed algorithms.

1. Introduction

Autonomous underwater vehicles (AUVs) play an important role in ocean surveying and monitoring. To perform underwater tasks perfectly, it is necessary to design a robust control to perform precise trajectory and attitude tracking that makes the AUV cruise on a planned path with pre – defined attitudes (Rezazadegan et al., 2015; Geranmehr and Nekoo, 2015). Performing precise attitude control of an AUV is a formidable task because of model nonlinearities, unknown hydrodynamic coefficients, and time – varying disturbances.

Various control methods have been proposed for AUVs while considering the aforementioned technical difficulties. For the model uncertainties, neural network (NN) – based adaptive control (Li et al., 2004, 2002; Chu et al., 2016; He et al., 2016), robust control and sliding mode control have been proposed. In Li et al. (2002), a two – layer neural network is applied to approximate the nonlinear uncertainties in the AUV dynamics. A predictor – based neural dynamic surface control is presented for the containment control of AUVs in Peng et al. (2015), in which the unknown dynamics of each AUV is identified by prediction error – based updating laws. In Li et al. (2004), a semi – globally stable neural network adaptive control scheme is presented for autonomous diving control of an AUV, where the smooth unknown dynamics of the vehicle is approximated by a NN. In Peng et al. (2015), the uncertain nonlinear dynamics of the vehicle is approximated via a neural network, and the unmeasurable states are constructed by a local observer. To address the model uncertainty and time – varying disturbances problem, an adaptive robust online constructive fuzzy control employing an online constructive fuzzy approximator is proposed in Wang et al. (2015), and a predictor – based neural dynamic surface control is designed in Peng et al. (2014). The radial basis function neural network is employed to design an adaptive control for systems subjected to unknown hysteresis and external disturbances in Chen and Ge (2015). A robust adaptive control is designed for an underwater remotely operated vehicle in Li et al. (2012), in which the barrier Lyapunov function is employed in Lyapunov syntheses to prevent the velocity constraint violation. In general, the payload and dynamics of an AUV will change when performing different tasks; thus, robust control is desired for control of the AUV when it experiences different angles of attack, sideslip or external disturbances. Robust control, such as sliding mode control, is proposed to attenuate the effects of external disturbances (Ashrafiuon et al., 2008; He et al., 2014; Dougherty et al., 1988; Chu and Zhang, 2014). In Dougherty et al. (1988), the AUV control is designed using sliding mode control due to its robust capacity, and a sea trial is performed

☆This work was supported by the National Natural Science Foundation of China (NSFC) under grants 61472325, 51209174 and 51311130137, the Natural Science Basic Research Plan in Shaanxi Province of China under grant 2015JM5254, and the Fundamental Research Funds for Central Universities under grant 3102015BJ014.
* Corresponding author.
E-mail address: r.cui@nwpu.edu.cn (R. Cui).

http://dx.doi.org/10.1016/j.oceaneng.2016.06.041
0029-8018/

using such a control approach. In Annamalai et al. (2015), a robust model predictive control for an unmanned surface vehicle is designed to handle sudden changes in system dynamics.

A dead–zone commonly exists in the actuator of a physical system. For an AUV, rudders always suffer from a small dead–zone, which can cause severe deterioration of the system performance and destroy the control precision. In most physical components of control systems, the parameters of the dead–zone are unknown. It is necessary to consider inputting the dead–zone into the control design. Several control strategies have been proposed. One of the methods for the control of the dead–zone is to design an adaptive dead–zone inverse (Tao and Kokotovic, 1994). In Deng et al. (2015), a smooth dead–zone inverse is used to compensate the effect of the input dead–zone, which has been employed in the backstepping controller design. Another method to address the input dead–zone is to model the dead zone as a time–varying disturbance–like term. In Wang et al. (2004), a robust adaptive control is proposed for a class of continuous–time nonlinear dynamic systems preceded by a dead–zone. This robust adaptive control scheme is developed without constructing a dead–zone inverse by using a new description of a dead–zone and by showing the properties of this dead–zone model intuitively and mathematically. In Ibrir et al. (2007), an adaptive tracking of systems with non–symmetric dead–zone characteristics is discussed with minimal knowledge of the dead–zone parameters. The proposed adaptive scheme requires only information of the bounds of the dead–zone slopes and treats the time–varying input coefficient as system uncertainties. In Roopaei et al. (2010), a robust adaptive fuzzy sliding mode control scheme is proposed to overcome the synchronization problem for a class of unknown nonlinear chaotic gyros. The parameters of the dead–zone are unknown; however, it only considered the symmetrical dead–zone. In Hua et al. (2015), an adaptive fuzzy control is designed for a class of uncertain nonlinear systems with an unknown function and unknown symmetric dead–zone input. In a recent work (Liu and Tong, 2015; Liu et al., 2016), the nonaffine pure–feedback discrete–time nonlinear system with dead–zone input is considered, where the systems are transformed into an n–step–ahead predictor and an adaptive compensative term is constructed to compensate for the dead–zone parameters.

Another technical challenge for AUV attitude control is the input saturation caused by physical actuators. The undesirable control input saturation will influence the stability of the control system and even make the entire system unstable. There are two main strategies to solve the actuator saturation. One is the direct design method (Gilbert and Tan, 1991), and the other is the anti–windup design method (Kothare et al., 1994). The so–called direct design is that actuator saturation is taken into account to make the closed–loop system stable when designing a controller. In Fischer et al. (2014), a direct method is used to solve the problem of input saturation based on the robust integral of the sign of the error (RISE). In Li et al. (2015), disturbance observers are designed to compensate for the disturbance caused by unknown input saturation, fuzzy approximation errors and other uncertain disturbances to solve the problem using the fuzzy approbation–based control. The anti–windup design ignores actuator saturation and design a linear controller that satisfies the performance specifications, and then an anti–windup compensator is designed to reduce the influence of saturation. In Kothare et al. (1994), a unified framework for studying the anti–windup design was proposed. In Chen et al. (2009), an adaptive tracking control for ocean surface vessels subjected to input saturation was presented based on a neural network and an anti–windup compensator.

In this paper, robust adaptive attitude controllers for AUV with unknown model parameters, external disturbances and input nonlinearities are presented based on sliding–mode control. The model of non–symmetric dead–zone nonlinearity with unknown parameters in Ibrir et al. (2007) is employed to address the input dead–zone. We model the non–symmetric dead–zone with unknown parameters as a time–varying disturbance–like term. To compensate for the effect of the input dead–zone, internal uncertainties and external disturbances, adaptation laws are designed to obtain parameter estimations, including the terms related to unknown dead–zone parameters, and other unknown model parameters via adaptive control and sliding mode control strategies. In addition, an anti–windup compensator is introduced to reduce the influence of actuator saturation.

The reminder of this paper is organized as follows. Section 2 presents the nonlinear model of AUVs and the attitude control problem. In Section 3, we design an adaptive controller for AUVs based on sliding mode only considering the unknown model parameters and disturbances. In Section 4, we design the controls for the unknown dead–zone and saturation. The simulation results are presented in Section 5, followed by experimental results in Section 6. Conclusions are drawn in Section 7.

2. Problem formulation

2.1. Motion equations

In this section, the dynamical model of a slender body AUV is briefly introduced. There two commonly used frames, namely, inertia–referenced frame and body–referenced frame, to describe the motion of an AUV. As shown in Fig. 1, the AUV used in this work is centered at the center of buoyancy (CB) and has the body–referenced x–axis forward, z–axis to port (left), and y–axis up. Looking forward from the bridge of the body, roll (φ) about the x–axis is positive counterclockwise, yaw (ψ) about the y–axis is positive turning left, and pitch (θ) about the z–axis is positive bow–up. In general, the model in $3D$ can be divided into three lightly interacting subsystems for the horizontal plane, vertical plane and roll. We also provide a simple view in the horizontal plane in Fig. 1, where the body–axis and inertia–axis frames are related through rotations about the y–axis with the yaw angle ψ. The sideslip angle is defined by $\beta = \arctan(v_z/\sqrt{v_x^2 + v_y^2})$, and the angle of attack is defined by $\alpha = -\arctan(v_y/v_x)$.

Through the coordinate frame transition, the kinematics of the AUV is described as

$$\begin{bmatrix} \dot{x} \\ \dot{y} \\ \dot{z} \end{bmatrix} = \begin{bmatrix} \cos\theta\cos\psi & \sin\psi\sin\varphi - \sin\theta\cos\psi\cos\varphi & \sin\psi\cos\varphi + \sin\theta\cos\psi\sin\varphi \\ \sin\theta & \cos\theta\cos\varphi & -\cos\theta\sin\varphi \\ -\cos\theta\sin\psi & \cos\psi\sin\varphi + \sin\theta\sin\psi\cos\varphi & \cos\psi\cos\varphi - \sin\theta\sin\psi\sin\varphi \end{bmatrix} \begin{bmatrix} v_x \\ v_y \\ v_z \end{bmatrix} \tag{1}$$

$$\begin{bmatrix} \dot{\psi} \\ \dot{\theta} \\ \dot{\varphi} \end{bmatrix} = \begin{bmatrix} 0 & \sec\theta\cos\varphi & -\sec\theta\sin\varphi \\ 0 & \sin\varphi & \cos\varphi \\ 1 & -\tan\theta\cos\varphi & \tan\theta\sin\varphi \end{bmatrix} \begin{bmatrix} \omega_x \\ \omega_y \\ \omega_z \end{bmatrix} \tag{2}$$

where $\omega_x, \omega_y, \omega_z$ are the angle velocity in the body-referenced frame.

The AUV dynamics includes nonlinear and coupled hydrodynamic parameters, which makes it difficult to design the control algorithm using the nonlinear model directly. The simplified dynamics model of the AUV neglecting the nonlinear coupling among different planes can be described as

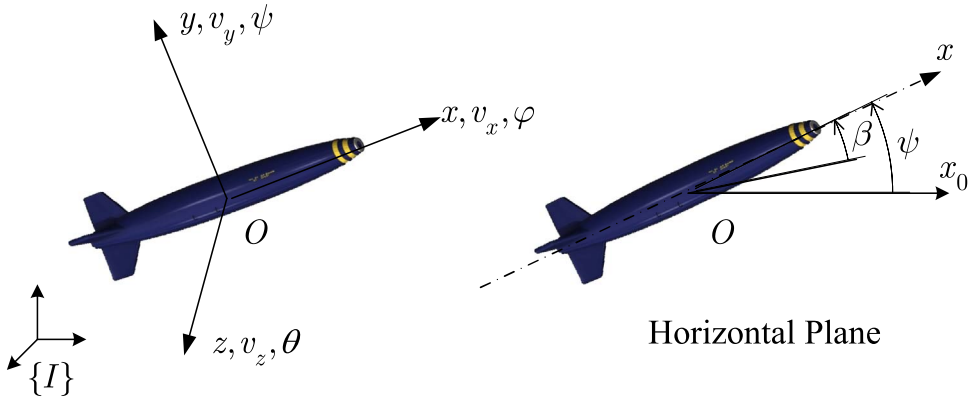

Fig. 1. Body-referenced coordinate system on an AUV.

$$
\begin{aligned}
(m+\lambda_{11})\dot{v}_x &= T - \tfrac{1}{2}C_{xS}\rho v^2 S - \Delta G\sin\theta \\
(m+\lambda_{22})\dot{v}_y &= -(mx_c+\lambda_{26})\dot{\omega}_z - mv_x\omega_z \\
&\quad + \tfrac{1}{2}\rho v^2 S(C_y^{\alpha}\alpha + C_y^{\delta_e}\delta_e + C_y^{\bar{\omega}_z}\bar{\omega}_z) - \Delta G\cos\theta\cos\varphi \\
(m+\lambda_{33})\dot{v}_z &= (mx_c-\lambda_{35})\dot{\omega}_y + mv_x\omega_y + \tfrac{1}{2}\rho v^2 S(C_z^{\beta}\beta + C_z^{\delta_r} + C_z^{\bar{\omega}_y}) \\
&\quad + \Delta G\cos\theta\sin\varphi \\
(J_{xx}+\lambda_{44})\dot{\omega}_x &= mv_x(y_c\omega_y + z_c\omega_z) \\
&\quad + \tfrac{1}{2}\rho v^2 SL(m_x^{\beta}\beta + m_x^{\delta_r}\delta_r + m_x^{\delta_d}\delta_d + m_x^{\bar{\omega}_x}\omega_x \\
&\quad + m_y^{\bar{\omega}_y}\omega_y) + G\cos\theta(y_c\sin\varphi + z_c\cos\varphi) + \Delta M_{xp} \\
(J_{yy}+\lambda_{55})\dot{\omega}_y &= -mv_x x_c\omega_y + (mx_c-\lambda_{35})\dot{v}_z \\
&\quad + \tfrac{1}{2}\rho v^2 SL(m_y^{\beta}\beta + m_y^{\delta_r}\delta_r + m_y^{\bar{\omega}_x}\bar{\omega}_x + m_y^{\bar{\omega}_y}\omega_y) \\
&\quad - G(x_c\cos\theta\sin\varphi + z_c\sin\theta) \\
(J_{zz}+\lambda_{66})\dot{\omega}_z &= -mv_x x_c\omega_z - (mx_c+\lambda_{26})\dot{v}_y \\
&\quad + \tfrac{1}{2}\rho v^2 SL(m_z^{\alpha}\alpha + m_z^{\delta_e}\delta_e + m_z^{\bar{\omega}_z}\bar{\omega}_z) \\
&\quad + G(y_c\sin\theta - x_c\cos\theta\cos\varphi)
\end{aligned} \tag{3}
$$

where m is the mass of the vehicle, ρ is the water density, $v=\sqrt{v_x^2+v_y^2+v_z^2}$ is the speed of the vehicle, λ_{ij}, $i, j = 1, \ldots, 6$ is the added mass, J_{xx}, J_{yy}, J_{zz} are the added moment of inertia, $r_{cg}=[x_c, y_c, z_c]^{\top}$ is the distance vector from the center of gravity to the center of buoyancy, and L and S are the length and the area of the maximum cross section, respectively. The hydrodynamic coefficients for drag, lift, and rudders are denoted as $C_*^{\#}$, where we omit the detailed expression for each symbol for simplification. The control inputs of the vehicle are the trust T, the steering rudder δ_r, the elevator δ_e and the differential rudder δ_d. For the control in the horizontal plane, vertical plane and the speed, there are several lightly interacting items in the simplified model.

2.2. Heading dynamics

The first three equations in (3) describe the dynamics of the vehicle velocity, and the last three denote the dynamics of the vehicle attitude. In general, the trust T is denoted as a constant, and the trajectory of the vehicle is controlled by adjusting the attitude of the vehicle using rudders while performing tasks using the slender body AUV. In this work, we focus on the attitude control of the AUV, particularly for the pitch and yaw angle. From the motion equations, we can find that the dynamics of the attitude can be written as a second-order system with nonlinear items and unknown hydrodynamics. In addition, the dynamics of yaw, pitch and roll have the same pattern. Thus, in the subsequent paragraph, we will take the heading control as an example to design the attitude control algorithm for a AUV, accompanied by a simulation and experimental results describing the control of all attitudes of an AUV.

In the design of the heading control, we neglect the vehicle's stable roll and assume that the vehicle has a small pitch angle. Considering disturbance and nonlinear items, the yaw dynamics and kinematics equations can be written as

$$
\begin{aligned}
\dot{\psi} &= \omega_y \\
\dot{\omega}_y &= c_1\omega_y + c_2\beta + c_3\delta_r + f(v, \psi, \omega_y, t) + d(t)
\end{aligned} \tag{4}
$$

where c_1 and c_2 are unknown parameters that depend on the hydrodynamics coefficients, c_3 is the open-loop control gain, $f(v, \psi, \omega_y, t)$ is a nonlinear item that includes the couplings with pitch and other motion parameters, d is the unknown disturbance acting on the vehicle, and δ_r is the control input. The model can be written in a compact form as

$$
\begin{aligned}
\dot{\psi} &= \omega_y \\
\dot{\omega}_y &= h^{\top}\Phi + c_3\delta_r + D
\end{aligned} \tag{5}
$$

where $h=[c_1, c_2]^{\top}$, $\Phi=[\omega_y, \beta]^{\top}$, and D denotes the nonlinear dynamics and disturbance term.

The objective is to adjust the rudder δ_r to control the yaw angle ψ following the desired trajectory $\psi_d(t)$ as time goes to infinity, i.e., the tracking error $e=\psi(t)-\psi_d(t)\to 0$, $t\to\infty$.

The time derivative of the tracking error can be written as

$$
\dot{e} = \dot{\psi} - \dot{\psi}_d = \omega_y - \dot{\psi}_d \tag{6}
$$

To facilitate the control design, the following assumptions are made.

Assumption 1. ψ and $\dot{\psi}$ are measurable outputs. The time-varying term D is bounded satisfying $|D|\le\rho$, where ρ is an unknown upper bound and $\rho>0$.

Assumption 2. The control gain c_3 is unknown, but its sign and upper bound are known, satisfying $0<c_3<\bar{c}_3$, where $\bar{c}_3$ is a known positive constant.

3. Adaptive sliding-mode controller design without input nonlinearities

In this section, an adaptive sliding mode control is proposed for the AUV heading control with unknown disturbances taken into account.

Choose the following sliding mode surface:

$$s = \dot{e} + \lambda e, \tag{7}$$

where $\lambda > 0$ is a design parameter satisfying the Hurwitz conditions.

Substituting (6) into (7) yields

$$s = \omega_y - \dot{\psi}_d + \lambda(\psi - \psi_d) \tag{8}$$

The time derivative of (8) is

$$\dot{s} = \dot{\omega}_y - \ddot{\psi}_d + \lambda(\omega_y - \dot{\psi}_d) \tag{9}$$

Substituting (5) into (9), we have

$$\dot{s} = h^{\top}\Phi + c_3\delta_r + D - \ddot{\psi}_d + \lambda(\omega_y - \dot{\psi}_d) \tag{10}$$

The accessibility of the sliding mode condition guarantees that any original state in space can reach the sliding mode surface in finite time, whereas it has no restriction during the approach course $s \to 0$. Hence, we introduce the exponential reaching law to improve the dynamic response of the system.

The exponential reaching law is chosen as (Gao and Hung, 1993)

$$\dot{s} = -\tau s - k\,\mathrm{sgn}(s) \tag{11}$$

where $\tau > 0$ and $k > 0$. A large τ will force states to approach the sliding mode surface with a high speed. Moreover, a large k will make the states of the system converge to the origin with a high speed. However, a large k will cause bad chattering to occur. Therefore, we should choose a large τ and a small k to guarantee a large approach rate and simultaneously reduce the chattering.

The control law can be selected as

$$\delta_r = b\left[-\tau s - k\,\mathrm{sgn}(s) - h^{\top}\Phi - \rho\,\mathrm{sgn}(s) + \ddot{\psi}_d - \lambda(\omega_y - \dot{\psi}_d)\right] \tag{12}$$

where $b = 1/c_3 > 0$.

Because h, b, and ρ are all unknown, we replace them with their estimations $\hat{h}$, $\hat{b}$, and $\hat{\rho}$, respectively. Then, the control law is proposed as

$$\delta_r = \hat{b}\left[-\tau s - k\,\mathrm{sgn}(s) - \hat{h}^{\top}\Phi - \hat{\rho}\,\mathrm{sgn}(s) + \ddot{\psi}_d - \lambda(\omega_y - \dot{\psi}_d)\right] = \hat{b}L \tag{13}$$

where $L = -\tau s - k\,\mathrm{sgn}(s) - \hat{h}^{\top}\Phi - \hat{\rho}\,\mathrm{sgn}(s) + \ddot{\psi}_d - \lambda(\omega_y - \dot{\psi}_d)$. $\hat{h}$, $\hat{b}$, and $\hat{\rho}$ are the estimations of h, b, and ρ, respectively.

The adaptation laws are chosen as

$$\begin{cases} \dot{\hat{h}} = k_1\Phi s \\ \dot{\hat{b}} = -k_2 L s \\ \dot{\hat{\rho}} = k_3|s| \end{cases} \tag{14}$$

where k_1, k_2, and k_3 are design positive parameters.

The stability of the closed-loop system will be proofed via Lyapunov analysis.

Theorem 1. *Consider the heading control system of an AUV (5) with sliding mode surface (7), closed-loop signals can be driven onto the sliding surface* $\lim_{t\to\infty} s(t) = 0$ *and errors converge to zero with the control law (13) and adaption laws (14).*

Proof. Consider the following Lyapunov function candidate:

$$V = \frac{1}{2}s^2 + \frac{1}{2k_1}\tilde{h}^{\top}\tilde{h} + \frac{1}{2k_2 b}\tilde{b}^2 + \frac{1}{2k_3}\tilde{\rho}^2 \tag{15}$$

where $\tilde{h}^{\top} = \hat{h}^{\top} - h^{\top}$, $\tilde{b} = \hat{b} - b$, and $\tilde{\rho} = \hat{\rho} - \rho$ are estimation errors.

Its time derivative can be written as

$$\begin{aligned} \dot{V} &= s\dot{s} + \frac{1}{k_1}\tilde{h}^{\top}\dot{\hat{h}} + \frac{1}{k_2 b}\tilde{b}\dot{\hat{b}} + \frac{1}{k_3}\tilde{\rho}\dot{\hat{\rho}} \\ &= s\dot{s} + \frac{1}{k_1}\tilde{h}^{\top}\dot{\hat{h}} + \frac{1}{k_2 b}\tilde{b}\dot{\hat{b}} + \frac{1}{k_3}\tilde{\rho}\dot{\hat{\rho}} \end{aligned} \tag{16}$$

Substituting (10) into (16), we have

$$\dot{V} = s\left[h^{\top}\Phi + c_3\delta_r + D - \ddot{\psi}_d + \lambda(\omega_y - \dot{\psi}_d)\right] + \frac{1}{k_1}\tilde{h}^{\top}\dot{\hat{h}} + \frac{1}{k_2 b}\tilde{b}\dot{\hat{b}} + \frac{1}{k_2}\tilde{\rho}\dot{\hat{\rho}} \tag{17}$$

With the control law (13) and the adaptation laws (14), we have

$$\begin{aligned} \dot{V} \le\ & -\tau s^2 - k|s| + |D \parallel s| - \hat{\rho}|s| + \tilde{\rho}|s| = -\tau s^2 - k|s| + |D \parallel s| \\ & - \rho|s| \le -\tau s^2 - k|s| \end{aligned} \tag{18}$$

Thus, $\dot{V} < 0$ for all $s \neq 0$. According to Barbalat's Lemma (Slotine and Li, 1991), $s \to 0$ as $t \to \infty$. The state trajectories can be driven to the sliding surface $\lim_{t\to\infty} s(t) = 0$. The closed-loop errors converge to zero, and the system achieves asymptotic stability. This completes the proof. □

Note that due to $\mathrm{sgn}(\cdot)$, the control will cause undesirable chattering. In practical usage, a boundary layer is always be introduced to solve the problem. The introduction of the boundary layer can reduce chattering; however, it is at the cost of stability and robustness. The $\mathrm{sgn}(s)$ in control law δ_r will be replaced by $\mathrm{sat}(s)$ in this work:

$$\mathrm{sat}(s) = \begin{cases} 1, & s > \phi \\ 1/\phi, & |s| \le \phi \\ -1, & s < -\phi \end{cases} \tag{19}$$

where ϕ is the boundary layer.

4. Control design with input nonlinearities

In practical applications for underwater vehicles, the rudder always has nonlinearities, including saturation and dead-zones, which can severely degrade the closed-loop system performance and even cause instability. It is necessary to design a controller that takes these nonlinearities into account to achieve the desired performance. In this section, we redesign the adaptive controller based on the results in the previous section. We divide the controller design into two steps. We only consider the dead-zone in the first step, and then we consider both the input saturation and dead-zone nonlinearities.

4.1. Dead-zone model

First, we consider the case with a dead-zone, ignoring the input saturation based on the given dynamics. The control input with a dead-zone, as shown in Fig. 2, is described as

$$\delta_r = m_{(u)}u + \sigma_{(u)} \tag{20}$$

where u is the control signal to be designed:

$$m_{(u)} = \begin{cases} m_r, & u > 0 \\ m_l, & u \le 0 \end{cases} \tag{21}$$

$$\sigma_{(u)} = \begin{cases} -m_l b_l, & u \le -b_l \\ -m_u u, & -b_l < u \le b_r \\ m_r b_r, & u \ge b_r \end{cases} \tag{22}$$

where m_r and m_l denote the right and the left slopes of the dead-zone characteristic, respectively. b_r and b_l represent the widths of the dead-zone.

For convenience, in the following paragraph, we simplify $m_{(u)}$ and $v_{(u)}$ as m, and σ, respectively. Based on the dead-zone model (20), the nonlinear dynamic system (5) can be rewritten as

$$\begin{aligned}\dot{\psi} &= \omega_y \\ \dot{\omega}_y &= h^{\top}\Phi + c_3 m u + c_3\sigma + D\end{aligned} \tag{23}$$

The following assumption is made for this problem:

Assumption 3. m_r, m_l, b_l and b_r are strictly positive and unknown. The bound of the characteristic slopes $m_{\max}$ is unknown. σ is bounded, satisfying $0 < |\sigma| \le \varpi$, where $\varpi = \max\{m_{\max} b_r, m_{\max} b_l\}$ with $m_{\max} = \max\{m_r, m_l\}$.

4.2. Disturbance observer

To reduce the tracking errors caused by disturbances and uncertainty and to reduce the chattering, we first design a disturbance observer.

Define the disturbance observer error as

$$\tilde{D} = \hat{D} - D \tag{24}$$

Because there is no prior information about the derivative of disturbance, it is reasonable to assume that the disturbance is slowly time varying, i.e.,

$$\dot{D} = 0 \tag{25}$$

The nonlinear disturbance observer is designed as follows:

$$\begin{cases}\dot{\hat{D}} = -k_{06}(\hat{\omega}_y - \omega_y) \\ \dot{\hat{\omega}}_y = \hat{D} + \hat{\mu}u + \hat{g} + \hat{h}^{\top}\Phi - k_{07}(\hat{\omega}_y - \omega_y)\end{cases} \tag{26}$$

where $\mu = mc_3$ and $g = c_3\sigma$. $\hat{\mu}$ and $\hat{g}$ are the estimations of μ and g, respectively. k_{06} and k_{07} are positive parameters to be designed.

4.3. Control design for input dead zone

We still choose the sliding mode surface as (7); then, its derivative becomes

$$\dot{s} = h^{\top}\Phi + mc_3 u + c_3\sigma + D - \ddot{\psi}_d + \lambda(\omega_y - \dot{\psi}_d) \tag{27}$$

Based on the exponential reaching law as (11), the control law is designed as

$$u = \hat{b}_1 L_1 \tag{28}$$

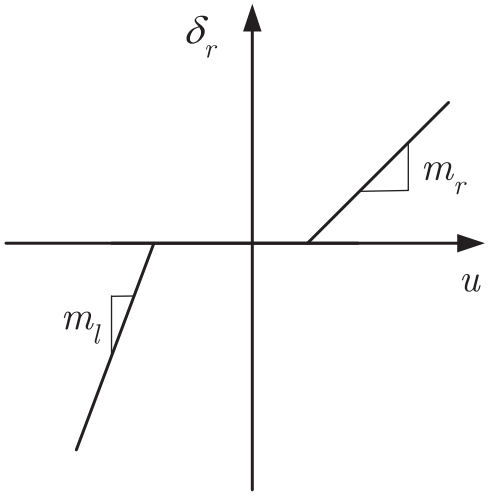

Fig. 2. Non-symmetric dead-zone of the rudder.

where $b_1 = 1/\mu = 1/(mc_3) > 0$ and $L_1 = -\tau s - k\,\mathrm{sgn}(s) - \hat{\rho}\,\mathrm{sgn}(s) - \hat{g} - \hat{h}^{\top}\Phi - \hat{D} + \ddot{\psi}_d - \lambda(\omega_y - \dot{\psi}_d)$.

The estimation errors are defined as $\tilde{h} = \hat{h} - h$, $\tilde{b}_1 = \hat{b}_1 - b_1$, $\tilde{\rho} = \hat{\rho} - \rho$, $\tilde{g} = \hat{g} - g$, $\tilde{\mu} = \hat{\mu} - \mu$, and $\tilde{\omega}_y = \hat{\omega}_y - \omega_y$.

Then,

$$\begin{aligned}\dot{s} &= h^{\top}\Phi + \frac{u}{b_1} + c_3\sigma + D - \ddot{\psi}_d + \lambda(\omega_y - \dot{\psi}_d) \\ &= h^{\top}\Phi + \frac{\hat{b}_1}{b_1}\left[-\tau s - k\,\mathrm{sgn}(s) - \hat{\rho}\,\mathrm{sgn}(s) - \hat{g} - \hat{h}^{\top}\Phi - \hat{D} + \ddot{\psi}_d - \lambda(\omega_y - \dot{\psi}_d)\right] \\ &\quad + c_3\sigma + D - \ddot{\psi}_d + \lambda(\omega_y - \dot{\psi}_d) \\ &= h^{\top}\Phi \\ &\quad + \left[1 + \frac{\tilde{b}_1}{b_1}\right]\left[-\tau s - k\,\mathrm{sgn}(s) - \hat{\rho}\,\mathrm{sgn}(s) - \hat{g} - \hat{h}^{\top}\Phi - \hat{D} + \ddot{\psi}_d\right. \\ &\quad \left. - \lambda(\omega_y - \dot{\psi}_d)\right] + c_3\sigma + D - \ddot{\psi}_d + \lambda(\omega_y - \dot{\psi}_d) \\ &= -\tau s - k\,\mathrm{sgn}(s) - \hat{\rho}\,\mathrm{sgn}(s) - \hat{g} - \tilde{h}^{\top}\Phi - \tilde{D} + c_3\sigma + \frac{\tilde{b}_1}{b_1}L_1\end{aligned} \tag{29}$$

The adaptation laws are chosen as

$$\begin{cases}\dot{\hat{h}} = k_{01}\Phi s - k_{01}\tilde{\omega}_y\Phi \\ \dot{\hat{b}}_1 = -k_{02}L_1 s \\ \dot{\hat{\rho}} = k_{03}|s| \\ \dot{\hat{g}} = k_{04}s - k_{04}\tilde{\omega}_y \\ \dot{\hat{\mu}} = -k_{05}\tilde{\omega}_y u\end{cases} \tag{30}$$

where k_{01}, k_{02}, k_{03}, k_{04}, and k_{05} are positive parameters to be designed.

Theorem 2. *Consider the AUV system (5), (20) with sliding mode surface (7), the closed-loop signals can be driven onto the sliding surface* $\lim_{t\to\infty} s(t) = 0$ *and errors converge to zero using the control law (28), adaption laws (30) and disturbance observer (26).*

Proof. Consider the following Lyapunov function candidate:

$$\begin{aligned}V = &\frac{1}{2}s^2 + \frac{1}{2k_{01}}\tilde{h}^{\top}\tilde{h} + \frac{1}{2k_{02}b_1}\tilde{b}_1^{\,2} + \frac{1}{2k_{03}}\tilde{\rho}^2 + \frac{1}{2k_{04}}\tilde{g}^2 + \frac{1}{2k_{05}}\tilde{\mu}^2 \\ &+ \frac{1}{2k_{06}}\tilde{D}^2 + \frac{1}{2}\tilde{\omega}_y^2\end{aligned} \tag{31}$$

Its time derivative is

$$\begin{aligned}\dot{V} = &s\dot{s} + \frac{1}{k_{01}}\tilde{h}^{\top}\dot{\tilde{h}} + \frac{1}{k_{02}b_1}\tilde{b}_1\dot{\tilde{b}}_1 + \frac{1}{k_{03}}\tilde{\rho}\dot{\tilde{\rho}} + \frac{1}{k_{04}}\tilde{g}\dot{\tilde{g}} + \frac{1}{k_{05}}\tilde{\mu}\dot{\tilde{\mu}} \\ &+ \frac{1}{k_{06}}\tilde{D}\dot{\tilde{D}} + \tilde{\omega}_y\dot{\tilde{\omega}}_y = s\dot{s} + \frac{1}{k_{01}}\tilde{h}^{\top}\dot{\hat{h}} + \frac{1}{k_{02}b_1}\tilde{b}_1\dot{\hat{b}}_1 + \frac{1}{k_{03}}\tilde{\rho}\dot{\hat{\rho}} \\ &+ \frac{1}{k_{04}}\tilde{g}\dot{\hat{g}} + \frac{1}{k_{05}}\tilde{\mu}\dot{\hat{\mu}} + \frac{1}{k_{06}}\tilde{D}\dot{\hat{D}} + \tilde{\omega}_y(\dot{\hat{\omega}}_y - \dot{\omega}_y)\end{aligned} \tag{32}$$

Substituting (29) and (30) into (32), we have

$$\begin{aligned}\dot{V} = &-\tau s^2 - k|s| - \hat{\rho}|s| - \tilde{g}s - \tilde{D}s + c_3\sigma s - \tilde{\omega}_y\tilde{h}^{\top}\Phi + \tilde{\rho}|s| \\ &+ \tilde{g}s - \tilde{g}\tilde{\omega}_y - \tilde{\mu}\tilde{\omega}_y u - \tilde{D}(\hat{\omega}_y - \omega_y) \\ &+ \tilde{\omega}_y\left[\tilde{h}^{\top}\Phi + \tilde{\mu}u + \tilde{g} + \tilde{D} - k_{07}\tilde{\omega}_y\right] \le -\tau s^2 \\ &- k|s| - k_{07}\tilde{\omega}_y^2 \le -\tau s^2 - k|s|\end{aligned} \tag{33}$$

Thus, $\dot{V} < 0$ for all $s \neq 0$. Based on Barbalat's lemma (Slotine and Li, 1991), $s \to 0$ as $t \to \infty$. This implies that the system achieves asymptotic stability and that the error converges to zero

asymptotically. This completes the proof.□

4.4. Control design with input saturation

Now, we consider the case with actuator saturation. When the computed control input reaches its bound, we will design an anti-windup compensator to reduce the influence of saturation.

The control input with actuator saturation is shown in Fig. 3. We can describe the saturation as

$$\delta_r = \mathrm{sat}(u) \tag{34}$$

where u is the designed control input, δ_r is the actual control input generated by the actuator, and $\mathrm{sat}(\cdot)$ denotes the nonlinear saturation characteristic, which can be written as

$$\delta_r = \mathrm{sat}(u) = \begin{cases} \delta_{rm}, & u > \delta_{rm} \\ u, & -\delta_{rm} \le u \le \delta_{rm} \\ -\delta_{rm}, & u < -\delta_{rm} \end{cases} \tag{35}$$

where δ_{rm} is the upper bound of the actuator.

To solve the problem of attitude control subjected to actuator saturation, we employ an anti-windup compensator as (Chen et al., 2009; Galeani et al., 2009)

$$\dot{w} = \begin{cases} -k^* w - \dfrac{|\bar{c}_3 s \Delta u| + \frac{1}{2}(\Delta u)^2}{|w|^2} w + \Delta u, & |w| \ge \iota \\ 0, & |w| < \iota \end{cases} \tag{36}$$

where $\Delta u = \delta_r - u$, w is the state of the auxiliary design system, $k^* > 0$ is a design parameter, and ι is a small positive constant. The yaw control of an AUV with an anti-windup compensator is shown in Fig. 4.

Considering the actuator saturation, the control is proposed as

$$u = \hat{b} L_2 \tag{37}$$

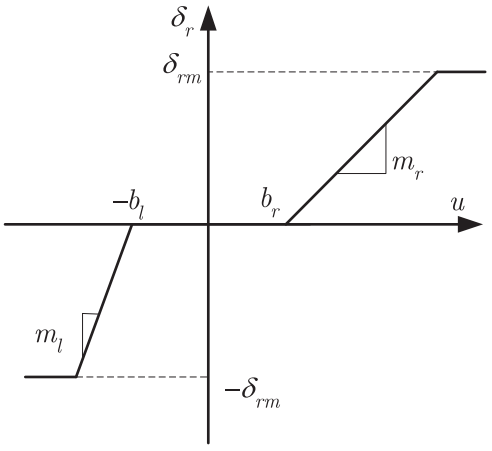

Fig. 3. Rudder saturation.

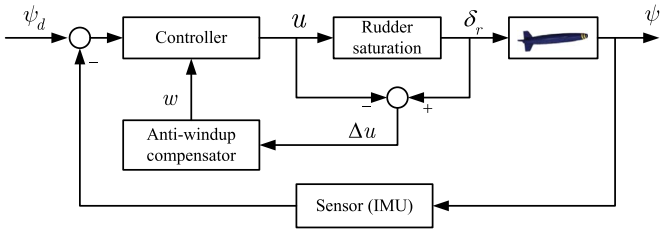

Fig. 4. Auxiliary system compensation (Galeani et al., 2009).

where $b = 1/c_3 > 0$, $L_2 = -\tau(s - w) - k\,\mathrm{sgn}(s) - \hat{\rho}\,\mathrm{sgn}(s) - \hat{h}^{\top}\Phi - \hat{D} + \ddot{\psi}_d - \lambda(\omega_y - \dot{\psi}_d)$.

The disturbance observer is designed as

$$\begin{cases} \dot{\hat{D}} = -k_{06}(\hat{\omega}_y - \omega_y) \\ \dot{\hat{\omega}}_y = \hat{D} + \hat{c}_3 \delta_r + \hat{h}^{\top}\Phi - k_{07}(\hat{\omega}_y - \omega_y) \end{cases} \tag{38}$$

where k_{06} and k_{07} are design positive parameters.

By choosing the sliding mode surface (7), the adaptation laws are designed as

$$\begin{cases} \dot{\hat{h}} = k_{01}\Phi s - k_{01}\tilde{\omega}_y \Phi \\ \dot{\hat{b}} = -k_{02} L_2 s \\ \dot{\hat{\rho}} = k_{03}|s| \\ \dot{\hat{c}}_3 = -(\hat{\omega}_y - \omega_y)\delta_r \end{cases} \tag{39}$$

where k_{01}, k_{02}, and k_{03} are design positive parameters.

Theorem 3. *Consider the AUV system (5), (35) with sliding mode surface (7), the closed-loop signals can be driven onto the sliding surface* $\lim_{t\to\infty} s(t) = 0$ *and errors converge to zero with the control law (37), adaption laws (39) and disturbance observer (38) based on the anti-windup compensator (36).*

Proof. Consider the following Lyapunov function candidate:

$$V = \frac{1}{2}s^2 + \frac{1}{2k_{01}}\tilde{h}^{\top}\tilde{h} + \frac{1}{2k_{02}b}\tilde{b}^2 + \frac{1}{2k_{03}}\tilde{\rho}^2 + \frac{1}{2}\tilde{c}_3^2 + \frac{1}{2}w^2 + \frac{1}{2k_{06}}\tilde{D}^2 + \frac{1}{2}\tilde{\omega}_y^2 \tag{40}$$

Its time derivative is

$$\begin{aligned} \dot{V} = {} & s\dot{s} + \frac{1}{k_{01}}\tilde{h}^{\top}\dot{\hat{h}} + \frac{1}{k_{02}b}\tilde{b}\dot{\hat{b}} + \frac{1}{k_{03}}\tilde{\rho}\dot{\hat{\rho}} + \tilde{c}_3\dot{\hat{c}}_3 + w\dot{w} + \frac{1}{k_{06}}\tilde{D}\dot{\hat{D}} \\ & + \tilde{\omega}_y(\dot{\hat{\omega}}_y - \dot{\omega}_y) = s\left[h^{\top}\Phi + c_3\delta_r + D - \ddot{\psi}_d + \lambda(\omega_y - \dot{\psi}_d)\right] \\ & + \frac{1}{k_{01}}\tilde{h}^{\top}\dot{\hat{h}} + \frac{1}{k_{02}b}\tilde{b}\dot{\hat{b}} + \frac{1}{k_{03}}\tilde{\rho}\dot{\hat{\rho}} + \tilde{c}_3\dot{\hat{c}}_3 + w\dot{w} + \frac{1}{k_{06}}\tilde{D}\dot{\hat{D}} \\ & + \tilde{\omega}_y(\dot{\hat{\omega}}_y - \dot{\omega}_y) \end{aligned} \tag{41}$$

Considering $\Delta u = \delta_r - u$ and (36), the above equation can be re-written as

$$\begin{aligned} \dot{V} = {} & s\left[h^{\top}\Phi + c_3(\Delta u + u) + D - \ddot{\psi}_d + \lambda(\omega_y - \dot{\psi}_d)\right] + \frac{1}{k_{01}}\tilde{h}^{\top}\dot{\hat{h}} \\ & + \frac{1}{k_{02}b}\tilde{b}\dot{\hat{b}} + \frac{1}{k_{03}}\tilde{\rho}\dot{\hat{\rho}} + \tilde{c}_3\dot{\hat{c}}_3 - k^* w^2 - |\bar{c}_3 s\Delta u| \\ & - \frac{1}{2}(\Delta u)^2 + \Delta u w + \frac{1}{k_{06}}\tilde{D}\dot{\hat{D}} + \tilde{\omega}_y(\dot{\hat{\omega}}_y - \dot{\omega}_y) \end{aligned} \tag{42}$$

Thus,

$$\begin{aligned} \dot{V} \le {} & s\left[h^{\top}\Phi + c_3 u + D - \ddot{\psi}_d + \lambda(\omega_y - \dot{\psi}_d)\right] + \frac{1}{k_{01}}\tilde{h}^{\top}\dot{\hat{h}} + \frac{1}{k_{02}b}\tilde{b}\dot{\hat{b}} \\ & + \frac{1}{k_{03}}\tilde{\rho}\dot{\hat{\rho}} + \tilde{c}_3\dot{\hat{c}}_3 - k^* w^2 - \frac{1}{2}(\Delta u)^2 + \Delta u w + \frac{1}{k_{06}}\tilde{D}\dot{\hat{D}} \\ & + \tilde{\omega}_y(\dot{\hat{\omega}}_y - \dot{\omega}_y) \end{aligned} \tag{43}$$

Substituting (5), (37), (38) and (39) into (43) obtains

$$\begin{aligned} \dot{V} \le {} & -\tau s^2 + \tau s w - k|s| - \rho|s| - \tilde{D}s - k^* w^2 - \tfrac{1}{2}(\Delta u)^2 + \Delta u w \\ & - k_{07}\tilde{\omega}_y^2 \end{aligned} \tag{44}$$

Because of these facts,

$$sw \le \frac{1}{2}(s^2 + w^2) \tag{45}$$

$$\Delta uw \le \frac{1}{2}(\Delta u^2 + w^2) \tag{46}$$

Substituting (45) and (46) into (44), we obtain

$$\begin{aligned}\dot{V} &\le -\tau s^2 + \frac{\tau}{2}\left[s^2 + w^2\right] - k|s| - \left[k^* - \frac{1}{2}\right]w^2 - k_{07}\tilde{\omega}_y^2 \\ &= -\frac{\tau}{2}s^2 - k|s| - \left[k^* - \frac{\tau}{2} - \frac{1}{2}\right]w^2 - k_{07}\tilde{\omega}_y^2 \le -\frac{\tau}{2}s^2 - k|s|\end{aligned} \tag{47}$$

where the design parameters are chosen to satisfy the condition $k^* - \frac{\tau}{2} - \frac{1}{2} > 0$.

According to Barbalat's Lemma (Slotine and Li, 1991), the state trajectories can be driven to the sliding surface $\lim_{t\to\infty} s(t) = 0$. The closed-loop errors converge to zero, and the system achieves asymptotic stability. This completes the proof.□

5. Simulation results

In this section, simulations are performed on the attitude stabilization problem of an AUV to demonstrate the performance of the adaptive sliding-mode controllers proposed in this paper.

Consider the AUV model with nominal model parameters $c_1 = -4.695$, $c_2 = 10.735$, $c_3 = 1.8207$, $c_4 = 0.2623$, $c_5 = -1.274$, $c_6 = -0.102$, and $h = [-4.695, 10.735]^T$. The initial states of the AUV are set as $\psi(0) = 10°$ and $\omega_y(0) = 3°/s$. The initial conditions of the estimated parameters are selected as $\hat{h}(0) = [-1, 2]^T$, $\hat{\rho}(0) = 0.5$, $\hat{b}(0) = 0$, $\hat{g}(0) = 0$, $\hat{\mu}(0) = 0$, $\hat{\omega}_y(0) = 0$, $\hat{D}(0) = 0.6$, and $\hat{c}_3(0) = 0$. The desired heading is a square wave that has been processed by a filter, and the amplitude of the square wave is 28.7°. The external disturbance is chosen as $d = 0.55\sin(0.01t) + 0.33\sin(0.1t) + 0.25\cos(0.02t) + 0.3\sin(0.1t)\cos(0.2t)$. The actuator saturation nonlinearity is characterized by the parameter $u_m = 12°$. The parameters of the dead-zone are $m_l = 0.3$, $m_r = 0.12$, $b_r = 1$, and $b_l = 1.3$. The saturation nonlinearity is characterized by the parameter $\delta_{r,\max} = 12°$.

We use three different controllers to control the attitude of the AUV, namely, traditional PID control, sliding mode control without considering the input saturation, and sliding mode with an anti-windup compensator considering the input saturation. The PID control for the AUV is designed as $u_{\text{pid}} = -k_p e - k_i \int_0^t e dt - k_d \dot{e}$, where $k_p = 4$, $k_i = 0.01$, and $k_d = 9$. The parameters in the sliding mode controller with an anti-windup compensator are selected as $\tau = 20$, $k = 0.02$, $k^* = 20$, $\lambda = 1$, $k_1 = k_2 = k_3 = k_{01} = k_{02} = k_{03} = k_{04} = k_{05} = 60$ and $k_{06} = k_{07} = 1$.

The simulation results are shown in Figs. 5–9. As shown, the adaptive sliding-mode controller performs better than the designed PID controller. In Fig. 5, the adaptive sliding-mode controller with an anti-windup compensator achieves better performance in heading control than the controller without a compensator and the PID controller. As shown in Fig. 7, the sliding mode control input without a compensator always hits the bound of the actuator and suffers from a chattering. This chattering is reduced by using a disturbance observer. This implies that the sliding mode based control can be used to address the model uncertainties and external disturbances while the input chattering is involved. For practical use, we should carefully select the control parameters and employ some methods to reduce chattering, such as a disturbance observer. In addition, due to the absence of persistent excitation, we cannot guarantee that the estimated value of a parameter converges to the real value.

6. Experimental results

In this section, we provide experimental results on an AUV whose attitudes are controlled by four separate rudders with x-type rudders, as shown in Fig. 10. The relationship between the

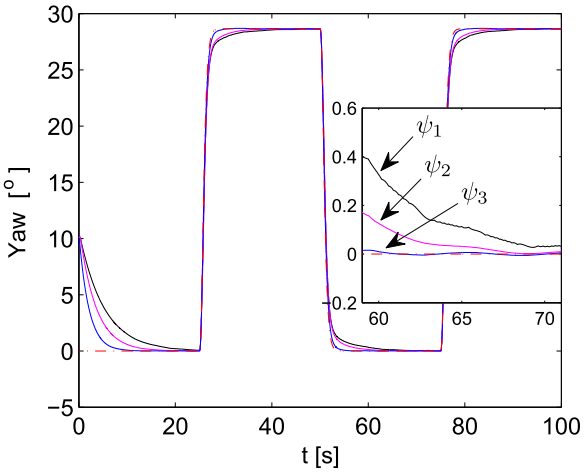

Fig. 5. Yaw output. ψ_1: PID control, ψ_2: Sliding-mode control without anti-windup compensator, ψ_3: Sliding-mode control with anti-windup compensator.

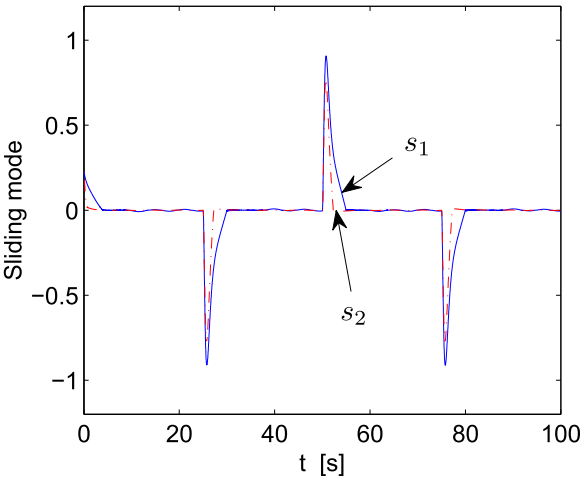

Fig. 6. Sliding mode surface. s_1: Without anti-windup compensator, s_2: With anti-windup compensator.

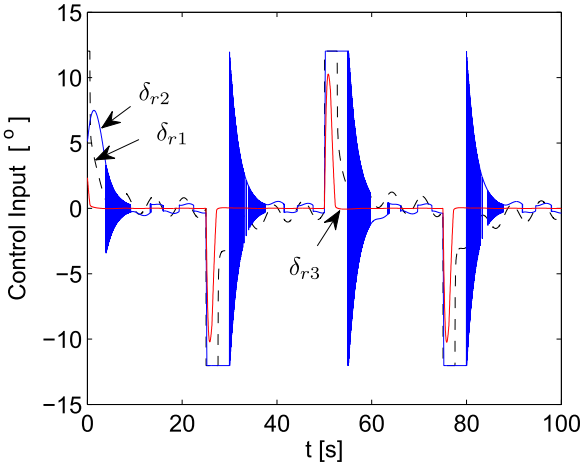

Fig. 7. Control input. δ_{r1}: PID control, δ_{r2}: Without anti-windup compensator, δ_{r3}: With anti-windup compensator.

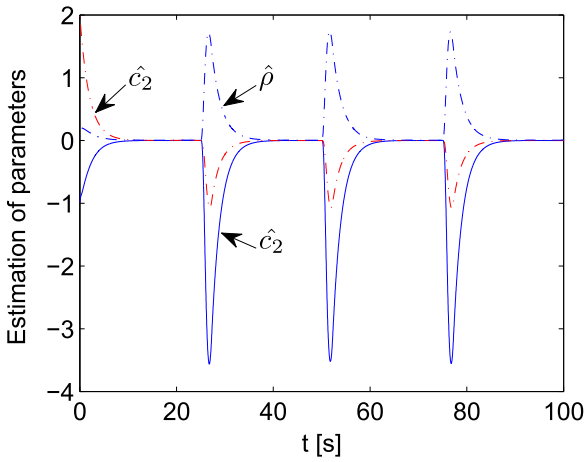

Fig. 8. Parameter estimation.

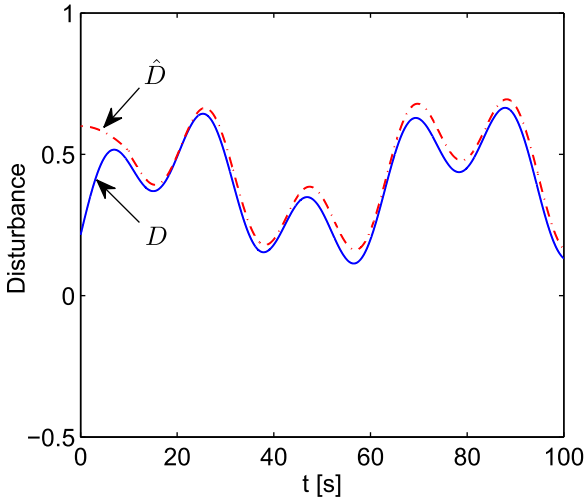

Fig. 9. Disturbance estimation.

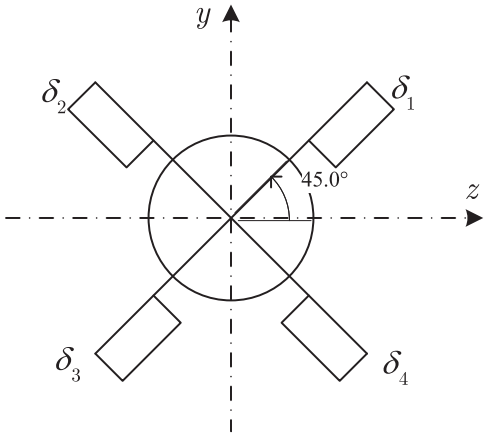

Fig. 10. Rudder configuration of the AUV in the experiment.

rudders δ_i, $i = 1, 2, 3, 4$, and the control inputs δ_r, δ_e and δ_d used in this work can be written as

$$\begin{bmatrix} \delta_e \\ \delta_r \\ \delta_d \end{bmatrix} = \begin{bmatrix} 1 & 1 & 1 & 1 \\ 1 & -1 & 1 & -1 \\ 1 & -1 & -1 & 1 \end{bmatrix} \begin{bmatrix} \delta_1 \\ \delta_2 \\ \delta_3 \\ \delta_4 \end{bmatrix}, \quad \text{and} \quad \begin{bmatrix} \delta_1 \\ \delta_2 \\ \delta_3 \\ \delta_4 \end{bmatrix} = \begin{bmatrix} 1 & 1 & 1 \\ 1 & -1 & -1 \\ 1 & 1 & -1 \\ 1 & -1 & 1 \end{bmatrix} \begin{bmatrix} \delta_e \\ \delta_r \\ \delta_d \end{bmatrix} \tag{48}$$

The diameter and the length of the AUV are 200 mm and 2015 mm, respectively. The nominal hydrodynamic parameters of the AUV, which are calculated using a commercial CFD software, are shown in Table 1. The control system of the AUV contains the processing unit together with navigation sensors as an inertial measurement unit (IMU) and a depth sensor. For implementation of control, navigation, and mission control systems, the AUV runs a standard C program on a 1.1 GHz DSP platform. The sensor, including IMU and the depth sensor, updates its value every 0.001 s, and the control implements every 0.1 s. The AUV is initialized at a depth of 30 m under the water with $\psi(0) = 2.4°$, $\theta(0) = 0$ and $\varphi(0) = -2.2°$, and its desired trajectory is cruising at a depth of

Table 1
Nominal hydrodynamic coefficients of the AUV in the experiment.

Parameter	Value	Parameter	Value	Parameter	Value
C_{xS}^{α}	−0.45	T	540	ΔG	102
C_y^{α}	1.98	C_z^{β}	−1.92	m_x^{β}	−0.01
$C_y^{\delta e}$	4.62	$C_z^{\delta r}$	−5.89	$m_x^{\delta d}$	−0.04
$C_y^{\bar{\omega} z}$	0.67	$C_z^{\bar{\omega} y}$	−0.67	$m_x^{\bar{\omega} x}$	−0.15
m_y^{β}	−0.01	m_z^{α}	0.31	$m_x^{\bar{\omega} y}$	0.002
J_y	23.8	J_z	23.8	J_x	0.56

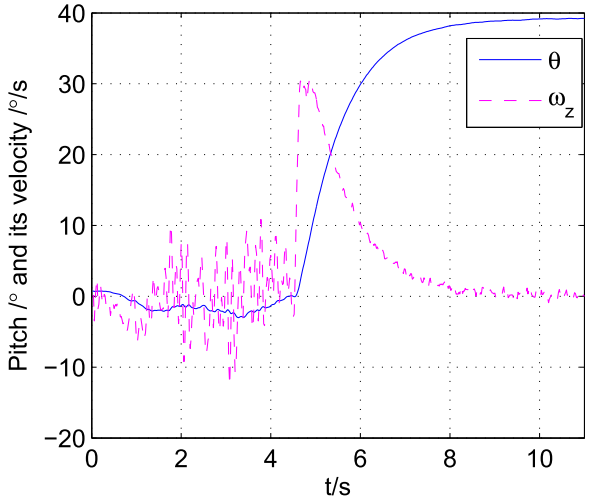

Fig. 11. Pitch of the AUV in the experiment.

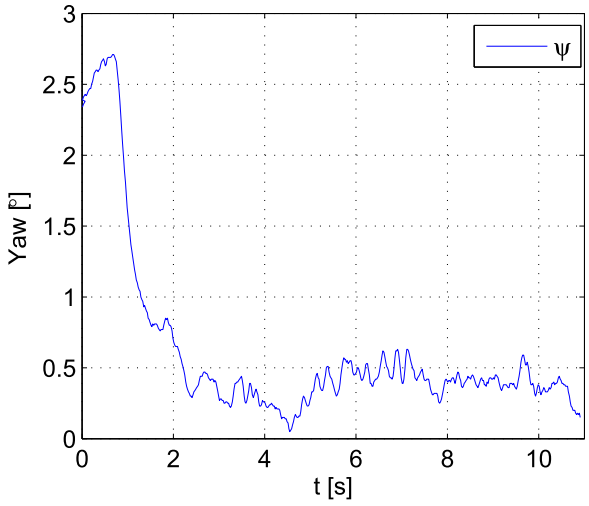

Fig. 12. Yaw of the AUV in the experiment.

30 m with desired yaw $\psi_d = 0$ for 4 s and then climbs to the water surface with desired pitch $\theta_d = 40^\circ$. The controller starts its control computation at 0.4 s and ends while the AUV climbs to the water surface. During the first 4 s for the AUV cruising the same depth, the depth controller is designed as $\delta_e = 0.25(y - y_d) + 0.1\dot{y} + 0.2\omega_z$. During the climbing, the AUV uses the controller designed in this work. For brevity, we design a simple PD controller for the roll of the AUV as $\delta_d = -0.5\varphi + 0.1\omega_x$.

The main purpose of the experiment is to validate the control design for the pitch and yaw channel using the proposed controller. The states of the AUV during the experiment are shown in Figs. 11– 14. To clearly show the control inputs of the AUV, we have calculated δ_e, δ_r and δ_d using (48), as shown in Fig. 15. From the experimental results, we can observe that the pitch error approaches a very small value near zero, and the yaw error can approach a small value near zero with some fluctuations. There is a fluctuation of the roll angle of the AUV and δ_d. This result means that the control design for the roll channel should be optimized by adjusting the control parameters or changing the control architecture to achieve better performance for the AUV.

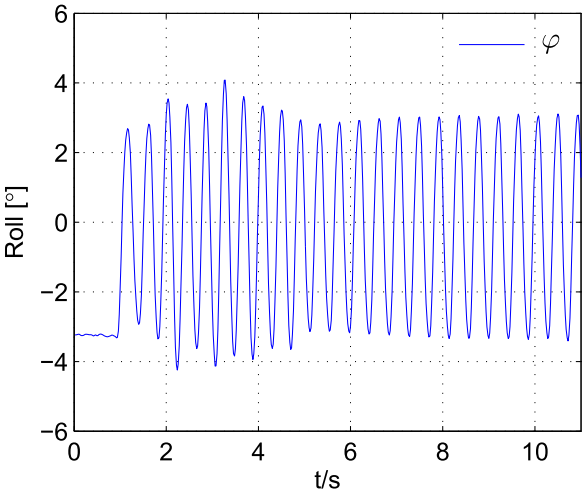

Fig. 13. Roll of the AUV in the experiment.

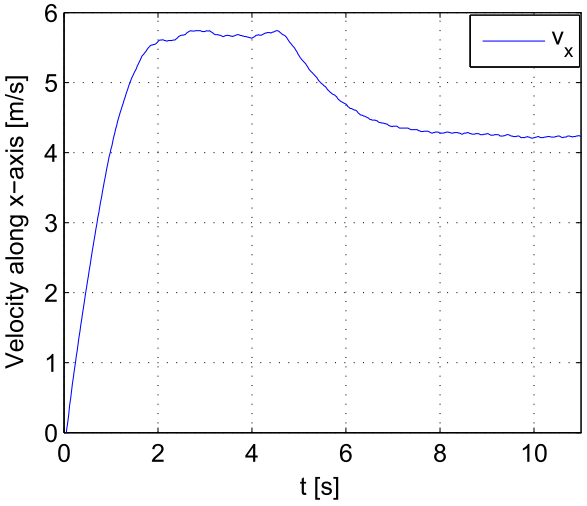

Fig. 14. Velocity of the AUV in the experiment.

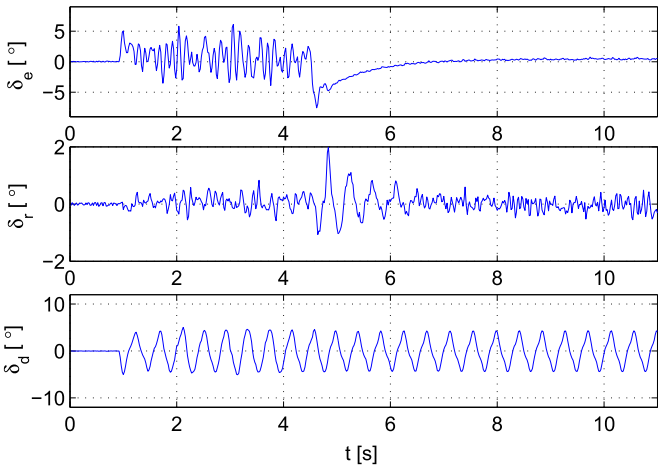

Fig. 15. Control inputs in the experiment.

7. Conclusion

In this paper, an adaptive dynamic anti-windup sliding mode attitude control based on a disturbance observer has been proposed for AUVs subjected to input nonlinearities. Based on the results without any input nonlinearities, the sliding-mode-based adaptive control has been designed for the case with an input nonsymmetric dead-zone with unknown parameters and with input saturation. Simulation results have been provided to compare with the PID controller and to show the effectiveness of the proposed approach. A simple experimental result has also been provided to validate the presented method. Further research will focus on the controller optimization and the practical utilization.

References

Annamalai, A.S.K., Sutton, Robert, Yang, C., Culverhouse, P., Sharma, S., 2015. Robust adaptive control of an uninhabited surface vehicle. J. Intell. Robot. Syst. 78 (2), 319–338.

Ashrafiuon, Hashem, Muske, Kenneth R., McNinch, Lucas C., Soltan, Reza A., 2008. Sliding-mode tracking control of surface vessels. IEEE Trans. Ind. Electron. 55 (November (11)), 4004–4012.

Chen, Mou, Ge, Shuzhi Sam, 2015. Adaptive neural output feedback control of uncertain nonlinear systems with unknown hysteresis using disturbance observer. IEEE Trans. Ind. Electron. 62 (12), 7706–7716.

Chen, Mou, Ge, Shuzhi Sam, Choo, Yoo Sang, 2009. Neural network tracking control of ocean surface vessels with input saturation. In: IEEE International Conference on Automation and Logistics, 2009, ICAL '09, pp. 85–89, August.

Chu, Zhenzhong, Zhang, Mingjun, 2014. Fault reconstruction of thruster for autonomous underwater vehicle based on terminal sliding mode observer. Ocean Eng. 88, 426–434.

Chu, Zhenzhong, Zhu, Daqi, Yang, Simon X., 2016. Observer-based adaptive neural network trajectory tracking control for remotely operated vehicle. IEEE Trans. Neural Netw. Learn. Syst. http://dx.doi.org/10.1109/TNNLS.2016.2544786.

Deng, Wenxiang, Yao, Jianyong, Ma, Dawei, 2015. Robust adaptive asymptotic tracking control of a class of nonlinear systems with unknown input dead-zone. J. Frankl. Inst. 352 (12), 5686–5707.

Dougherty, F., Sherman, T., Woolweaver, G., Lovell, G., 1988. An autonomous underwater vehicle (AUV) flight control system using sliding mode control. In: Proceedings of OCEANS '88. A Partnership of Marine Interests, Baltimore, MD, pp. 1265–1270, October.

Fischer, Normann, Kan, Zhen, Kamalapurkar, Rushikesh, Dixon, Warren E., 2014. Saturated rise feedback control for a class of second-order nonlinear systems. IEEE Trans. Autom. Control 59 (4), 1094–1099.

Galeani, Sergio, Tarbouriech, Sophie, Turner, Matthew, Zaccarian, Luca, 2009. A tutorial on modern anti-windup design. Eur. J. Control 15 (3), 418–440.

Gao, Weibing, Hung, James C., 1993. Variable structure control of nonlinear systems: a new approach. IEEE Trans. Ind. Electron. 40 (1), 45–55.

Geranmehr, Behdad, Nekoo, Saeed Rafee, 2015. Nonlinear suboptimal control of fully coupled non-affine six-DOF autonomous underwater vehicle using the state-dependent Riccati equation. Ocean Eng. 96, 248–257.

Gilbert, Elmer G., Tan, Kok Tin, 1991. Linear systems with state and control

constraints: the theory and application of maximal output admissible sets. IEEE Trans. Autom. Control 36 (9), 1008–1020.
He, Wei, Chen, Yuhao, Yin, Zhao, 2016. Adaptive neural network control of an uncertain robot with full-state constraints. IEEE Trans. Cybern. 46 (3), 620–629.
He, Wei, Zhang, Shuang, Ge, Shuzhi Sam, 2014. Robust adaptive control of a thruster assisted position mooring system. Automatica 50 (7), 1843–1851.
Hua, Jing, Li, Yi-Min, Zhang, Kun, Li, Pingping, 2015. Observer-based adaptive fuzzy control of a class of nonlinear systems with unknown symmetric nonlinear dead zone input. Appl. Math. Model. 40 (7), 4370–4379.
Ibrir, Salim, Xie, Wen Fang, Su, Chun-Yi, 2007. Adaptive tracking of nonlinear systems with non-symmetric dead-zone input. Automatica 43 (3), 522–530.
Kothare, Mayuresh V., Campo, Peter J., Morari, Manfred, Nett, Carl N., 1994. A unified framework for the study of anti-windup designs. Automatica 30 (12), 1869–1883.
Li, Ji Hong, Lee, Pan Mook, Jun, Bong Huan, 2004. Application of a robust adaptive controller to autonomous diving control of an AUV. In: 30th IEEE Annual Conference on Industrial Electronics Society, 2004, IECON 2004, vol. 1, pp. 419–424, November.
Li, Ji-Hong, Lee, Pan-Mook, Lee, Sang-Jeong, 2002. Motion control of an AUV using a neural network adaptive controller. In: Proceedings of the 2002 International Symposium on Underwater Technology, pp. 217–221.
Li, Zhijun, Su, Chun-Yi, Wang, Liangyong, Chen, Ziting, Chai, Tianyou, 2015. Nonlinear disturbance observer-based control design for a robotic exoskeleton incorporating fuzzy approximation. IEEE Trans. Ind. Electron. 62 (9), 5763–5775.
Li, Zhijun, Yang, Chenguang, Ding, Nan, Bogdan, Stjepan, Ge, Tong, 2012. Robust adaptive motion control for underwater remotely operated vehicles with velocity constraints. Int. J. Control Autom. Syst. 10 (2), 421–429.
Liu, Y.J., Gao, Y., Tong, S., Chen, C.L.P., 2016. A unified approach to adaptive neural control for nonlinear discrete-time systems with nonlinear dead-zone input. IEEE Trans. Neural Netw. Learn. Syst. 27 (January (1)), 139–150.
Liu, Yan-Jun, Tong, Shaocheng, 2015. Adaptive NN tracking control of uncertain nonlinear discrete-time systems with nonaffine dead-zone input. IEEE Trans. Cybern. 45 (3), 497–505.
Peng, Zhouhua, Wang, Dan, Shi, Yang, Wang, Hao, Wang, Wei, 2015. Containment control of networked autonomous underwater vehicles with model uncertainty and ocean disturbances guided by multiple leaders. Inf. Sci. 316, 163–179.
Peng, Zhouhua, Wang, Dan, Wang, Hao, Wang, Wei, 2014. Distributed coordinated tracking of multiple autonomous underwater vehicles. Nonlinear Dyn. 78 (2), 1261–1276.
Peng, Zhouhua, Wang, Dan, Zhang, Hongwei, Lin, Yejin, 2015. Cooperative output feedback adaptive control of uncertain nonlinear multi-agent systems with a dynamic leader. Neurocomputing 149, 132–141.
Rezazadegan, F., Shojaei, K., Sheikholeslam, F., Chatraei, A., 2015. A novel approach to 6-DOF adaptive trajectory tracking control of an AUV in the presence of parameter uncertainties. Ocean Eng. 107, 246–258.
Roopaei, Mehdi, Jahromi, Mansoor Zolghadri, John, Robert, Lin, Tsung-Chih, 2010. Unknown nonlinear chaotic gyros synchronization using adaptive fuzzy sliding mode control with unknown dead-zone input. Commun. Nonlinear Sci. Numer. Simul. 15 (9), 2536–2545.
Slotine, Jean-Jacques E., Li, Weiping, et al., 1991. Applied Nonlinear Control. Prentice-Hall, Englewood Cliffs, NJ.
Tao, Gang, Kokotovic, P.V., 1994. Adaptive control of plants with unknown dead-zones. IEEE Trans. Autom. Control 39 (January (1)), 59–68.
Wang, Ning, Er, Meng Joo, Sun, Jing-Chao, Liu, Yan-Cheng, 2015. Adaptive robust online constructive fuzzy control of a complex surface vehicle system. IEEE Trans. Cybern. http://dx.doi.org/10.1109/TCYB.2015.2451116.
Wang, Xing-Song, Su, Chun-Yi, Hong, Henry, 2004. Robust adaptive control of a class of nonlinear systems with unknown dead-zone. Automatica 40 (3), 407–413.